**Electronic supplementary materials** *Mendeleev Commun.*, 2020, **30**, 296-298

# 9*H*-Thioxanthen-9-one *S*,*S*-dioxide based redox active labels for electrochemical detection of DNA duplexes immobilized on Au electrodes

**Leonid A. Shundrin, Irina A. Os'kina, Irina G. Irtegova and Alexandr F. Poveshchenko**

## Table of Contents



## Section 1. Synthesis of thioxanthenones 1a-c and their sulfones 2a-d.

**General:** 2-Bromomethylthioxanthene-9-one was synthesized according to the procedures reported in the literature[1]. DCC, thiosalicylic acid were obtained from Sigma-Aldrich, N-hydroxysuccinimide was obtained from Fluka. $CH_3CN$ and DMF were purified in accordance with the standard procedure. Analytical and spectral measurements were carried out at Multi-Access Center *Chemical Service*, Siberian Branch of the Russian Academy of Sciences. Elemental analysis, HRMS, IR and NMR spectroscopy were used to identify the structures of synthesized compounds. IR spectra were measured using a Bruker Vector 22 spectrometer. The $^{1}H$, $^{13}C$ spectra were obtained with Bruker DRX-500, Bruker AV-300 and Bruker AV-400 spectrometers. High resolution MS spectra (EI, 70 eV) were obtained with DFS Thermo Electron instrument. Melting points were measured using a Mettler Toledo FD-900.

**General procedure**[2] **for the synthesis of 1a,b**: A mixture of anhydrous $K_2CO_3$ (0.10 g, 0.74 mmol) in 5 ml dry DMF was stirred at room temperature. Then 2-bromomethyl-9*H*-thioxanthene-9-one (0.11 g, 0.36 mmol) and 2-/4-mercaptobenzoic acid (0.06g, 0.39 mmol) were added to the mixture. The mixture was heated under stirring at 80°C for 2 h and cooled. The product was

filtered, washed with 10% HCl and ethanol, dried at room temperature. Then the residue was subjected to column chromatography over silica gel ($CHCl_3$) to give products **1a, b** in yields of 0.127g, 0.113 g (93%, 83%), respectively.

**2-((9-Oxo-9*H*-thioxanthen-2-yl)methylthio)benzoic acid (1a)**: white solid, 93%, mp 255.2 °C with dec. IR (KBr): 741, 1257, 1437, 1466, 1587, 1635, 1682, 3431 $cm^{-1}$. $^1H$ NMR (400 MHz, $DMSO_{d6}$): δ = 4.41 (s, 2H, $CH_2$), 7.21 (m, 1H), 7.51 (m, 2H), 7.59 (m, 1H), 7.78 (m, 1H), 7.84-7.89 (m, 4H), 8.46 (m, 1H), 8.54 (m, 1H) ppm. $^{13}C$ NMR (125.8 MHz, $DMSO_{d6}$): δ = 34.91, 124.22, 125.88, 126.63, 126.86, 126.89, 128.29, 128.32, 129.14, 129.21, 130.99, 132.33, 133.05, 133.86, 135.34, 135.96, 136.52, 140.51, 167.53, 178.66 ppm. HRMS (DFS) calcd for $C_{21}H_{14}O_3S_2$: 378.0379. Found: m/z 378.0382.

**4-((9-Oxo-9*H*-thioxanthen-2-yl)methylthio)benzoic acid (1b)**: white solid, 83%, mp 283.2 °C with dec. IR (KBr): 742, 1300, 1321, 1400, 1439, 1473, 1537, 1593, 1635, 1689, 3417 $cm^{-1}$. $^1H$ NMR (400 MHz, $DMSO_{d6}$): δ = 4.45 (s, 2H, $CH_2$), 7.31 (m, 2H), 7.57 (m, 1H), 7.76-7.81 (m, 6H), 8.46 (m, 2H), ppm. $^{13}C$ NMR (100.6 MHz, $DMSO_{d6}$): δ = 35.76, 126.50, 126.66, 126.73, 127.06, 128.21, 128.30, 128.85, 129.07, 132.91, 133.47, 135.18, 136.44, 136.64, 168.77, 178.59 ppm. HRMS (DFS) calcd for $C_{21}H_{14}O_3S_2$: 378.0379. Found: m/z 378.0385.

**Procedure for the synthesis of (1c, 2d)**: The mixture of 0.2 g acid **1a**, or 0.22g **2b** (0.5 mmol) with 0.07 g of *N*-hydroxysuccinimide (0.6 mmol) and 0.13 g of DCC (0.6 mmol) in 5 ml of $CH_3CN$ was stirred at 0°C for 7 h and 0.3 ml of triethylamine (1.9 mmol) was added to the mixture. Then 0.06 ml of isopropylamine (0.7 mmol) in 1 ml of $CH_3CN$ was added drop wise to the mixture. The reaction mixture was stirred for 2 h at room temperature. The precipitate was removed by filtration. Then the residue after filtrate evaporation was subjected to column chromatography over silica gel ($CHCl_3$) to afford products **1c**, **2d** in yields of 0.143g, 0.144 g (68%, 60%), respectively.

***N*-Isopropyl-2-((9-oxo-9*H*-thioxanthen-2-yl)methylthio)benzamide (1c)**: white solid, 68%, mp 164.4 °C with dec. IR (KBr): 741, 1072, 1117, 1302, 1435, 1589, 1628, 3269 $cm^{-1}$. $^1H$ NMR (400 MHz, $CDCl_3$): δ = 1.23 (d, *J* = 7.0 Hz, 6H, $2CH_3$), 4.21 (s, 2H, $CH_2$), 4.26 (q, *J* = 7.0 Hz, 1H, CH), 6.27 (m, 1H), 7.20-7.27 (m, 1H), 7.31-7.33 (m, 1H), 7.44-7.49 (m, 3H), 7.51-7.56 (m, 2H), 7.58-7.62 (m, 1H), 8.45 (m, 1H), 8.58 (m, 1H) ppm. $^{13}C$ NMR (100.6 MHz, $CDCl_3$): δ = 22.55, 39.12, 41.92, 125.92, 126.18, 126.26, 127.07, 128.54, 128.94, 128.99, 129.62, 129.77, 130.22, 131.73, 132.23, 132.68, 132.79, 135.70, 136.04, 137.05, 138.29, 167.19, 179.62 ppm. HRMS (DFS) calculated for $C_{24}H_{21}NO_2S_2$: 419.1008. Found: m/z 419.1000.

***N*-Isopropyl-4-((9-oxo-9*H*-thioxanthen-2-yl)methylsulfonyl)benzamide 10,10-dioxide (2d):** white solid, 60%, mp 211-212 °C. IR (KBr): 762, 1142, 1153, 1171, 1298, 1323, 1635, 1674, 3336

$cm^{-1}$. $^1H$ NMR (400 MHz, $DMSO_{d6}$): δ = 1.17 (d, *J* = 6.6 Hz, 6H, $2CH_3$, 4.10 (q, *J* = 7.1 Hz, 1H, CH)), 5.11 (s, 2H, $CH_2$), 7.82 (m, 1H), 7.88 (m, 2H), 7.97 (m, 1H), 8.03 (m, 2H), 8.07 (m, 1H), 8.18 (m, 1H), 8.23 (m, 1H), 8.29 (m, 1H), 8.51 (m, 1H) ppm. $^{13}C$ NMR (75.5 MHz, $DMSO_{d6}$): δ = 22.21, 59.44, 79.17, 123.42, 123.76, 128.13, 128.18, 129.02, 129.90, 129.94, 131.33, 134.05, 134.91, 135.65, 137.61, 139.65, 139.90, 140.0, 140.05, 163.88, 177.72 ppm. HRMS (DFS) calculated for $C_{24}H_{21}O_6NS_2$: 483.0805. Found: m/z 483.0809.

**General procedure for the synthesis of (2a-c):** Hydrogen peroxide (10 ml) was added to solution of compounds **1a-c** (0.36 mmol), in 30 ml of acetic acid and refluxed for 2.5 h. After cooling to room temperature reaction mixture was poured in water. Precipitate was filtered, washed with water and dried. Column chromatography over silica gel ($CHCl_3$) gives compounds **2a-c** in yields of 0.079 g, 0.108 g, 0.105 g (50%, 68%, 60%), respectively.

**2-((9-Oxo-9*H*-thioxanthen-2-yl)methylsulfonyl)benzoic acid 10,10-dioxide (2a):** white solid, 50%, mp 259-260°C. IR (KBr): 762, 1122, 1148, 1157, 1163, 1298, 1672, 1699, 1728, 3433 $cm^{-1}$. $^1H$ NMR (400 MHz, $DMSO_{d6}$): δ = 5.23 (s, 2H, $CH_2$), 7.61 (m, 1H), 7.68 (m, 1H), 7.79 (m, 2H), 7.86 (m, 1H), 7.96 (m, 1H), 8.06 (m, 1H), 8.15 (m, 1H), 8.21 (m, 2H), 8.28 (m, 1H) ppm. $^{13}C$ NMR (100.6 MHz, $DMSO_{d6}$): δ = 60.72, 123.53, 123.92, 129.15, 129.48, 129.96, 130.07, 131.37, 134.21, 134.63, 134.88, 135.43, 135.80, 137.82, 140.04, 140.10, 168.92, 177.79 ppm. HRMS (DFS) calculated for $C_{21}H_{14}O_7S_2$: 442.0175. Found: m/z 442.0168.

**4-((9-Oxo-9*H*-thioxanthen-2-yl)methylsulfonyl)benzoic acid 10,10-dioxide (2b):** white solid, 68%, mp 284.5°C with dec. IR (KBr): 760, 1124, 1148, 1162, 1232, 1304, 1674, 1730, 3425 $cm^{-1}$. $^1H$ NMR (400 MHz, $DMSO_{d6}$): δ = 5.13 (s, 2H, $CH_2$), 7.83 (m, 1H), 7.91 (m, 2H), 7.97 (m, 1H), 8.07 (m, 1H), 7.96 (m, 1H), 8.13 (m, 2H), 8.23 (m, 1H), 8.28 (m, 2H) ppm. $^{13}C$ NMR (100.6 MHz, $DMSO_{d6}$): δ = 59.43, 123.47, 123.82, 128.50, 129.03, 129.16, 129.89, 129.94, 130.09, 130.30, 131.31, 134.09, 135.67, 137.69, 139.95, 140.06, 166.41, 177.72 ppm. HRMS (DFS) calculated for $C_{21}H_{14}O_7S_2$: 442.0176. Found: m/z 442.0180.

***N*-Isopropyl-2-((9-oxo-9*H*-thioxanthen-2-yl)methylsulfonyl)benzamide 10,10-dioxide (2c):** white solid, 60%, mp 202-203°C. IR (KBr): 762, 1147, 1163, 1306, 1624, 1647, 1682, 3242$cm^{-1}$. $^1H$ NMR (300 MHz, $CDCl_3$): δ = 1.33 (d, *J* = 7.1 Hz, 6H, $2CH_3$), 4.33 (q, *J* = 7.1 Hz, 1H, CH), 5.00 (s, 2H, $CH_2$), 5.78 (m, 1H), 7.40 (m, 1H), 7.52 (m, 1H), 7.61 (m, 2H), 7.78 (m, 2H), 7.86 (m, 1H), 8.03 (m, 1H), 8.15 (m, 1H), 8.26 (m, 1H), 8.31 (m, 1H) ppm. $^{13}C$ NMR (125.8 MHz, $CDCl_3$): δ = 22.36, 42.62, 62.14, 123.43, 123.70, 128.14, 129.13, 129.77, 130.55, 130.71, 130.96, 131.56, 133.17, 134.07, 134.54, 134.57, 135.35, 136.91, 137.96, 140.71, 140.78, 167.55, 177.66 ppm. HRMS (DFS) calculated for $C_{24}H_{21}O_6NS_2$: 483.0805. Found: m/z 483.0800.

## Section 2. Synthesis and labelling of oligonucleotides

The model oligonucleotides were synthesized using ASM-800 DNA synthesizer (‘‘Biosset,’’ Novosibirsk, Russia). The base sequences in the 22-based complementary oligonucleotides for duplex formation (oligoprobe 1 with 3’-SH-anchor group and oligonucleotide 2 with 5’-aminolinker group) were the following:

HS-$(CH_2)_6$-3’-CCGTCTTCGATACGCTATACCC-5’ (oligoprobe 1)

$H_2N$-$(CH_2)_6$-5’-GGCAGAAGCTATGCGATATGGG-3’ (oligonucleotide 2).

Thiol-contaning modifier was introduced at the 3’-end of the oligonucleotide **1**. HS group served as an “anchor” to immobilize the oligoprobe 1 onto the pre-cleaned and golden modified surface of Au working electrodes. To label the oligonucleotide 2 with the redox active modifiers **2a, b**, the 5’-end of the oligonucleotide 2 was modified with an amino-link group (TFA amino-link CE reagent, PE Applied Biosystems, Foster City, CA). Both modifications were made during automated oligonucleotide synthesis.

*Labelling procedure of oligonucleotide 2*

Succinimide esters of **2a,b** were synthesized according to the described procedure[3] and used immediately for modifying the oligonucleotide **2**.

50 μl of 0.2M $[Et_3NH]HCO_3$ water buffer (pH=8.2) with 6 o.u. of 5’-end amino modified oligonucleotide 2 were mixed in Eppendorf tube. The tubes with oligonucleotide 2 in $[Et_3NH]HCO_3$ buffer and 30 μl of 0.1 M solution of the N-succinimide derivative of **2b (2a)** in DMF (for peptide synthesis) were placed in ice (t~0 $^oC$) for 5 min. Then the solvents in both tubes were united and mixed by pipette. The tube with reaction mixture was stirred at room temperature for 3 hours and remained overnight. At the next day the labelled oligoprobe 2 was purified by gel-filtration using Illustra NAP-5 Columns (GE Helthcare) with Sephadex G-25 DNA grade resin. The purification quality was controlled with spectrophotometer GE Healthcare Uvicord™ SII. Final concentration of the oligoprobe 2 was adjusted to 100 μM.

## Section 3. Cyclic voltammetry

*Cyclic voltammetric* measurements of **1a-c; 2a-d** were performed at 295 K in an argon atmosphere in DMF, DMF-$H_2O$ mixtures at a stationary Pt disk electrode ($S$ = 0.015 $cm^2$) with 0.1 M $Et_4NClO_4$ as a supporting electrolyte. Potential sweep rates were within a range of $0.1 < \nu < 1.5$ V $s^{-1}$. DMF was purified by a standard procedure. A PG 310 USB potentiostat (HEKA Elektronik GmbH, Germany) was used for CV measurements. A standard electrochemical cell (solution volume of 5 ml) connected to the potentiostat with a three-electrode scheme was used. Peak potentials are quoted with reference to a saturated calomel electrode (SCE). Pure resistance of the

cell (*R*) was measured with LCR meter INSTEK (Taiwan) with signal frequency of 1kHz and amplitude of 0.5 V. In DMF-$H_2O$ mixtures *R* varies from 800 Ω in DMF to 900 Ω in DMF-$H_2O$ (5:1).

CV measurements at various potential sweep rates (ν) were carried out with two types of potential sweep (TPS):

1) A triangular potential sweep without a time delay between cycles;

2) A triangular potential sweep with a 20s delay between each cycle.

For the second type, the Ar bubbling of the working solution was conducting during the delay, which led to the initial equilibrium conditions of the working electrode.

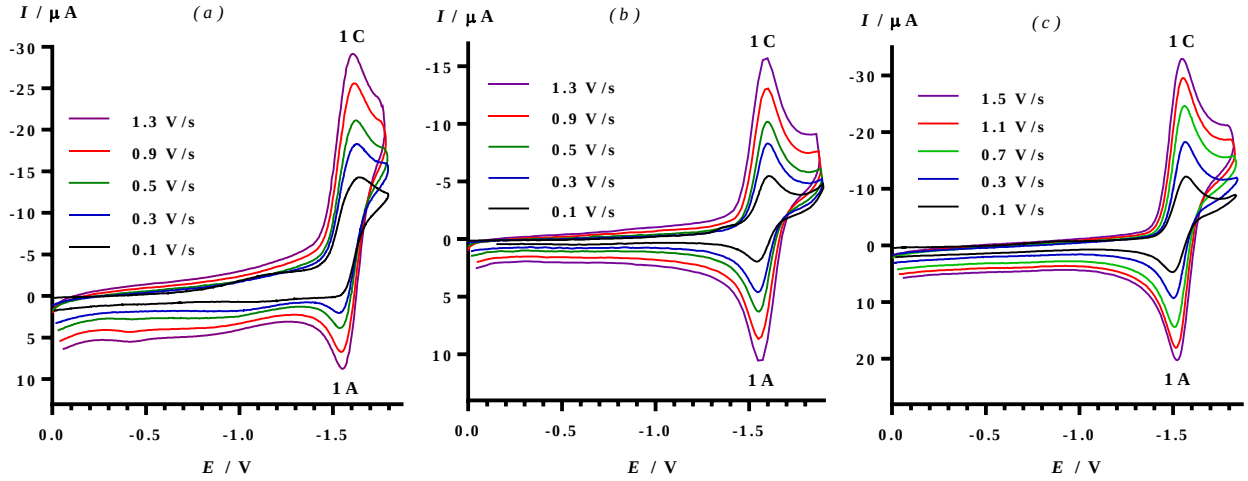


**Figure S1** CVs: (*a*) **1a** (2.4 mM), (*b*) **1b** (1.5 mM), (*c*) **1c** (2.6 mM) in DMF within potential sweep range 0.0>*E*>–1.9 V at various potential sweep rates (indicated by color). No Ar bubbling was conducted.

**CV studies of intermediate compounds 1a-c. (Notes to Figure S1**).

ECR of **1b,c** in DMF is a reversible one-electron process (E-process) characterised by a single diffusion-controlled CV-wave ($E_p^{1A} - E_p^{1C} = 0.06$ V, $I_p^{1A}/I_p^{1C} \approx 0.95$, ν = 0.1 V·s$^{-1}$)* (Figures S1(*b*,*c*), S2(*a*)). ECR of **1a** is an EC-process (Figure S1(*a*)). The corresponding CV-wave is irreversible at potential sweep rate ν=0.1 V s$^{-1}$ and becomes reversible at ν=0.9 V s$^{-1}$ (Figure S1(*a*)). In DMF-$H_2O$ mixture with molar fraction of $H_2O$ χ= 0.46, the reduction peaks of compounds **1a-c** are beyond the available potential range for this mixture (0 >*E*> –1.3 V), and are not observed.

* Designation of potentials $E_p^{ij}$ is the following: *i* is a number of peak, *j* = "C" or "A" indicates the cathode or anode branch of CV curve

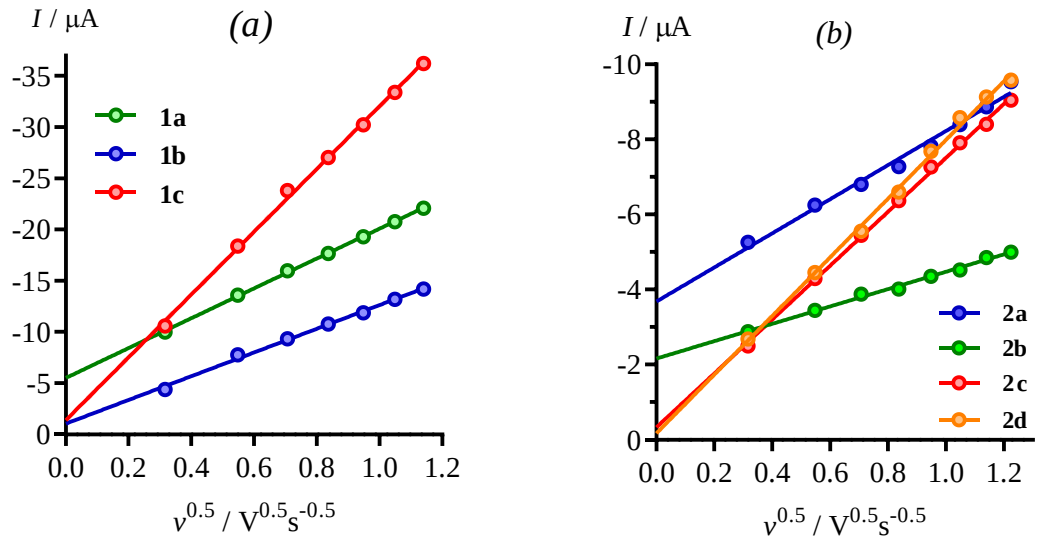


**Figure S2** The dependences of the peak 1C current on $v^{0.5}$ for compounds **1a-c** in DMF (*a*), and **2a-d** in DMF (*b*).

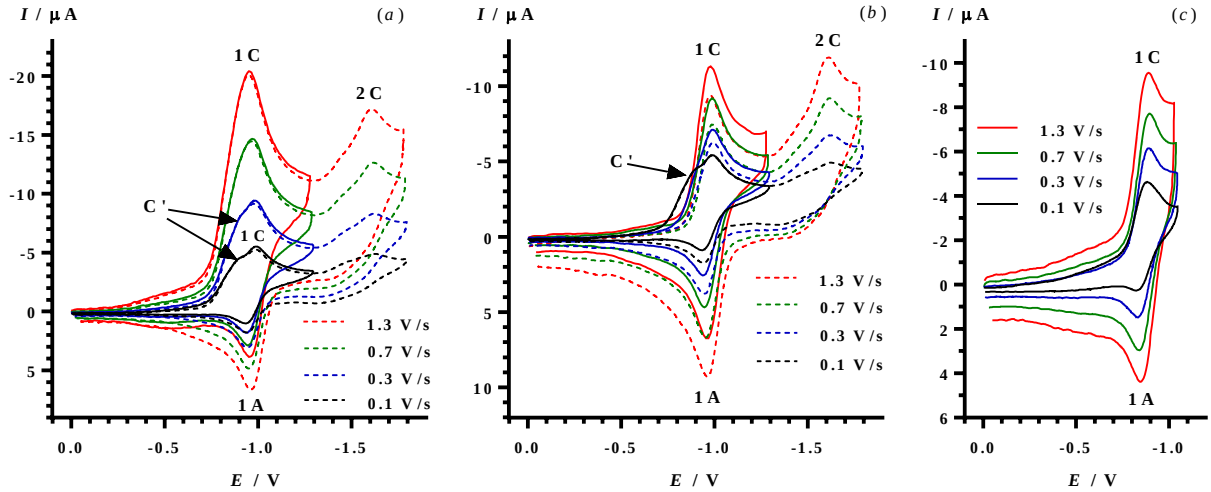


**Figure S3** CVs of **2a** (1.5 mM): (*a*) in DMF in potential sweep ranges 0 > *E* >–1.8 V (dotted line) and 0 > *E* >–1.3 V (solid line) with Ar bubbling before each cycle, (*b*) without Ar bubbling; (*c*) in DMF-$H_2O$ mixture with $H_2O$ molar fraction $\chi$=0.462.

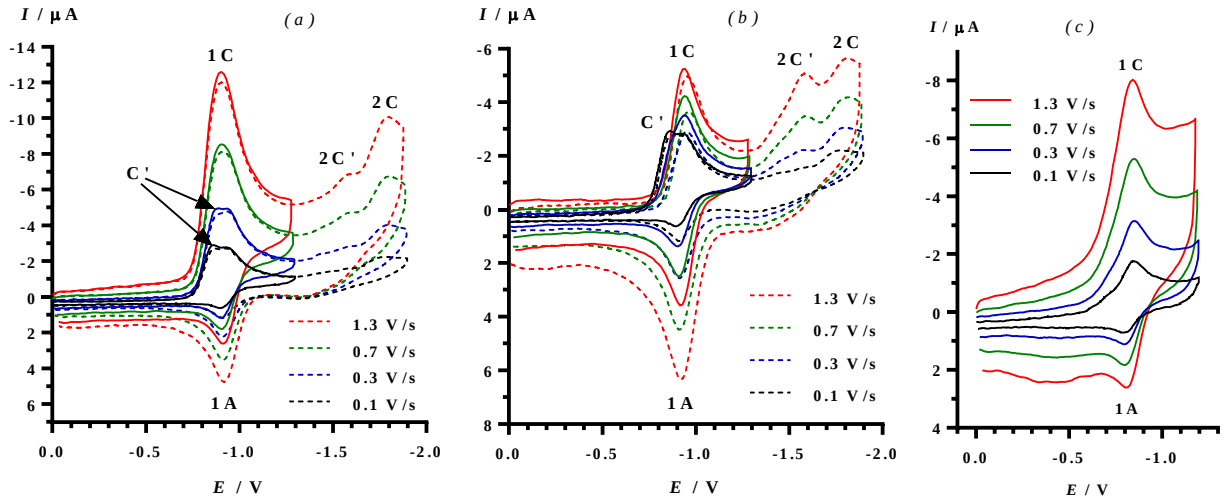


**Figure S4** CVs of **2b** (0.8 mM): (*a*) in DMF in potential sweep ranges 0 > *E* >–1.8 V (dotted line) and 0 > *E* >–1.3 V (solid line) with Ar bubbling before each cycle, (*b*) without Ar bubbling in DMF; (*c*) in DMF-$H_2O$ mixture with $H_2O$ molar fraction $\chi$=0.462.

**Notes to Figures S3, S4**.

An additional peak (C') is observed in the CVs of both acids **2a,b** at a potential close to the first reductive peak 1C, thus making the observed current of complex origin. CV measurements with increasing ν and Ar bubbling before each cycle showed a sharp increase in 1C current (Figures S3(*a*), S4(*a*)). However, an increase in 1C peak current with increasing ν became ordinary for a reversible peak at ν>0.1 V/s, if Ar bubbling was not applied (Figures S3(*b*), S4(*b*). In the latter case, $I_p^{1C}$ is not diffusion controlled only, since the corresponding dependences on $\nu^{0.5}$ don't pass through the origin (Figure S2(*b*)). Thus, we assume that pre-peak C' has an adsorption nature, probably due to the existence of a protolytic equilibrium of acids **2a,b** in DMF.

Note, that the one-electron and reversible nature of the first stage of ECR **2a,b** was confirmed by a combination of ECR **2a,b** with EPR spectroscopy, since the corresponding persistent radical anions (RA) of **2a,b** were observed (Section 4).

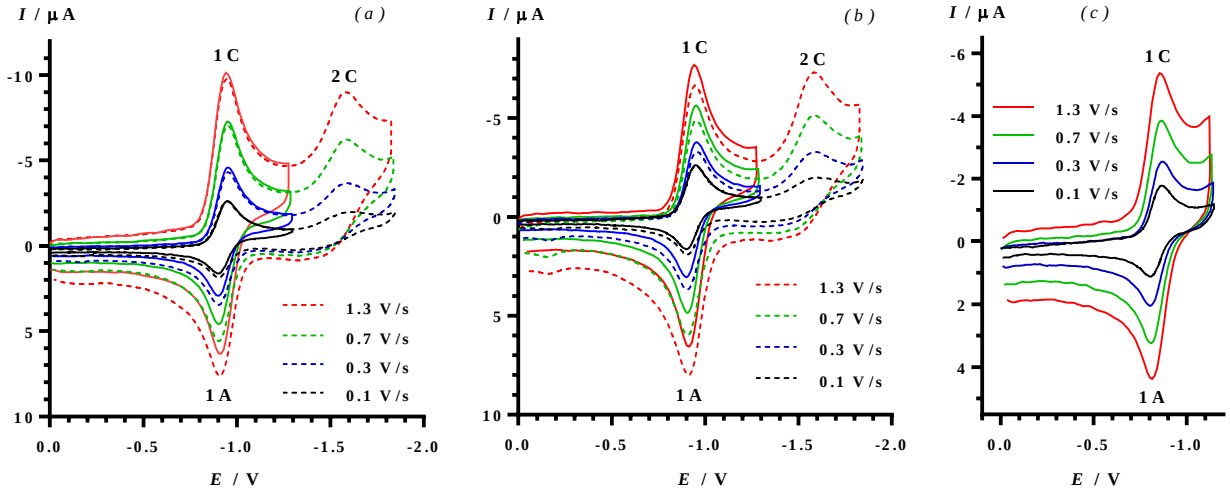


**Figure S5** CVs of **2c** (0.7 mM): (*a*) in DMF in potential sweep ranges 0 > *E* >–1.9 V (dotted line) and 0 > *E* >–1.3 V (solid line) with Ar bubbling before each cycle, (*b*) without Ar bubbling in DMF; (*c*) in DMF-$H_2O$ mixture with $H_2O$ molar fraction χ=0.462.

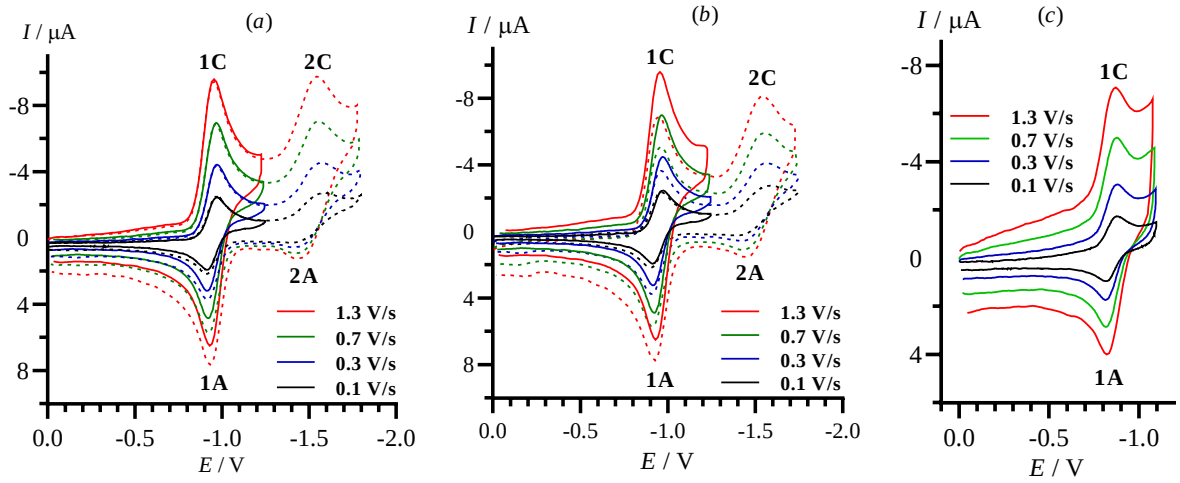


**Figure S6** CVs of **2d** (0.64 mM): (*a*) in DMF in potential sweep ranges 0 > *E* >–1.9 V (dotted line) and 0 > *E* >–1.3 V (solid line) with Ar bubbling before each cycle, (*b*) without Ar bubbling in DMF; (*c*) in DMF-$H_2O$ mixture with $H_2O$ molar fraction $\chi$=0.462.

**Notes to Figures S5, S6**.

The first stage of ECR of benzamides **2c,d** is a one-electron reversible and diffusion-controlled process in DMF and its mixtures with water (Figure S5, S6, S2(*b*)). Reversibility was confirmed by a combination of ECR **2c,d** with EPR spectroscopy (Section 4). Thus, the absence of free carboxyl group under the binding of **2a,b** via $NH_2$ group allows the additional processes observed for acids **2a,b** to disappear, indicating the possibility of their use as oligonucleotide modifiers.

**Table S1** Electrochemical CV cathodic ( $E_p^{iC}$ ) and anodic ( $E_p^{1A}$ ) peaks[a] and half-wave ( $E_{1/2}^1$ ) potentials for compounds **2a-d** in DMF.

| Compound | | **2a**[b] | **2b**[c] | **2c** | **2d** |
|---|---|---|---|---|---|
| $E_p^{iC}$, V | $i$ = 1 | –0.99 | –0.95 | –0.96 | –0.97 |
| | $i$ = 2 | –1.62 | –1.77 | –1.60 | –1.60 |
| $E_p^{1A}$,V | | –0.94 | –0.89 | –0.90 | –0.91 |
| $E_{1/2}^1$, V | | –0.97 | –0.94 | –0.93 | –0.94 |

[a] Measured with Pt working electrode *vs* SCE, $v$ = 0.1 V·s$^{-1}$; in potentials designation, $E_p^{iC}$, $i$ is a number of peak, symbol "C" indicates the cathode branch of the CV curve.

[b] The adsorptive peak C' at –0.92 V.

[c] The adsorptive peak C' at –0.87 V; the peak 2C' at –1.58 V revealed on 2nd and subsequent CV cycles.

**Table S2** Electrochemical CV cathodic ($E_p^{1C}$) and anodic ($E_p^{1A}$) peaks[a] and half-wave ($E_{1/2}^1$) potentials for benzoic acids **2a**,**b** in DMF and DMF–$H_2O$.

| $H_2O$ molar fraction ($\chi$) | **2a** | | | **2b** | | |
|---|---|---|---|---|---|---|
| | $E_p^{1C}$, V | $E_p^{1A}$, V | $E_{1/2}^1$, V | $E_p^{1C}$, V | $E_p^{1A}$, V | $E_{1/2}^1$, V |
| 0 | –0.992 | –0.941 | –0.966 | –0.945 | –0.889 | –0.917 |
| 0.147 | –0.970 | –0.906 | –0.938 | –0.900 | –0.860 | –0.880 |
| 0.256 | –0.930 | –0.884 | –0.907 | –0.883 | –0.838 | –0.861 |
| 0.340 | –0.912 | –0.862 | –0.887 | –0.869 | –0.821 | –0.845 |
| 0.408 | –0.903 | –0.835 | –0.869 | –0.858 | –0.802 | –0.830 |
| 0.462 | –0.889 | –0.827 | –0.858 | –0.850 | –0.792 | –0.821 |

[a] Measured with Pt working electrode *vs* SCE, $v = 0.1$ V·s$^{-1}$.

**Table S3** Electrochemical CV first cathodic ($E_p^{1C}$) and anodic ($E_p^{1A}$) peaks[a] and half-wave ($E_{1/2}^1$) potentials for *N*-isopropyl-benzamides **2c,d** in DMF and DMF–$H_2O$.

| $H_2O$ molar fraction ($\chi$) | **2c** | | | **2d** | | |
|---|---|---|---|---|---|---|
| | $E_p^{1C}$, V | $E_p^{1A}$, V | $E_{1/2}^1$, V | $E_p^{1C}$, V | $E_p^{1A}$, V | $E_{1/2}^1$, V |
| 0 | –0.955 | –0.900 | –0.927 | –0.970 | –0.908 | –0.939 |
| 0.147 | –0.928 | –0.865 | –0.897 | –0.950 | –0.886 | –0.918 |
| 0.256 | –0.907 | –0.844 | –0.876 | –0.931 | –0.864 | –0.898 |
| 0.340 | –0.896 | –0.826 | –0.861 | –0.922 | –0.846 | –0.884 |
| 0.408 | –0.880 | –0.810 | –0.845 | –0.895 | –0.828 | –0.862 |
| 0.462 | –0.870 | –0.800 | –0.835 | –0.883 | –0.820 | –0.852 |

[a] Measured with Pt working electrode *vs* SCE, $v = 0.1$ V·s$^{-1}$.

**Table S4** The dependences of the 1st reductive half-wave potential[a] of **2a-d** from $H_2O$ molar fraction ($E_{1/2}^1(\chi) = A\chi + B$)

| Comp. | A, V | B, V | R[b] | $E_{1/2}^1(\chi=1)$, V |
|---|---|---|---|---|
| **2a** | 0.245 | –0.970 | 0.998 | –0.725 |
| **2b** | 0.205 | –0.914 | 0.996 | –0.709 |
| **2c** | 0.198 | –0.927 | 0.999 | –0.729 |
| **2d** | 0.190 | –0.943 | 0.983 | –0.753 |

[a] Measured in DMF:$H_2O$ on Pt working electrode *vs* SCE with $v = 0.1$ V·s$^{-1}$;
[b] Correlation coefficient.

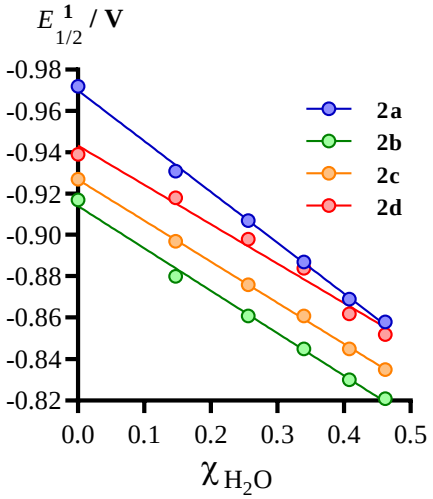


**Figure S7** Solvent dependences of $E_{1/2}^1$ in DMF-$H_2O$ mixtures.

## Section 4. EPR measurements

The EPR spectra of **2a-d** RAs were measured with an ELEXSYS E-540 spectrometer (X-band, MW frequency ~9.87 GHz, MW power 20 mW, modulation frequency 100 kHz, and modulation amplitude 0.006 mT) equipped with a high-Q cylindrical resonator ER4119HS. For the EPR measurements stationary ECR of compounds **2a-d** at the corresponding first peak potentials was carried out at 295 K under anaerobic conditions. Electrochemical cell for EPR measurements equipped with Pt working electrode was placed into the EPR cavity. Electrolysis of **2a-d** was performed in dry DMF with 0.1 M $Et_4NClO_4$ as a supporting electrolyte and in DMF-$H_2O$ mixture ($\chi$=0.46) with 0.05 M $Et_4NClO_4$ + 0.05 M $Me_4NClO_4$ as supporting electrolytes. Simulations of the experimental EPR spectra were accomplished with the *Winsim 2002* program.[4] The *Simplex* algorithm was used for optimization of hyperfine coupling (hfc) constants and line widths.

**Table S5** Experimental[a] isotropic hyperfine coupling (hfc) constants (G) of RAs, **2a-d** in DMF and DMF-$H_2O$ mixture ($\chi$ = 0.46)

| **RA** | Hfc constants (G) |
|---|---|
| **2a** | 1.64 (1), 2.95 (3), 0.68 (4), 0.78 (5), 2.74 (6), 0.17[b] (7), 1.77 (8), 0.14[b] ($CH_2$) |
| **2b** | 1.87 (1), 3.05 (3), 0.71 (4), 0.80 (5), 2.73 (6), 0.29 (7), 1.67 (8), 0.22 ($CH_2$) |
| | 1.97 (1), 3.19 (3), 0.75 (4), 0.75 (5), 2.87 (6), 0.36 (7), 2.00 (8), 0.23 ($CH_2$) |
| **2c** | 1.87 (1), 3.03 (3), 0.73 (4), 0.78 (5), 2.73 (6), 0.30 (7), 1.69 (8), 0.22 ($CH_2$) |
| | 2.01 (1), 3.19 (3), 0.74 (4), 0.82 (5), 2.87 (6), 0.36 (7), 1.96 (8), 0.22 ($CH_2$) |
| **2d** | 1.80 (1), 3.11 (3), 0.71 (4), 0.80 (5), 2.76 (6), 0.21 (7), 1.68 (8), 0.1[b] ($CH_2$) |
| | 2.03 (1), 3.26 (3), 0.77 (4), 0.85 (5), 2.82 (6), 0.38 (7), 2.06 (8), 0.24 ($CH_2$) |

[a] In DMF (in DMF – $H_2O$ ($\chi$ = 0.462), highlighted in gray), numbers of RAs correspond to those of their neutral precursors; numbers of atoms H are the same as for C atoms they are bound with, the hfc constants assignment is based on the data from the previous work[5].

[b] Unresolved hfc constants determined by simulation.

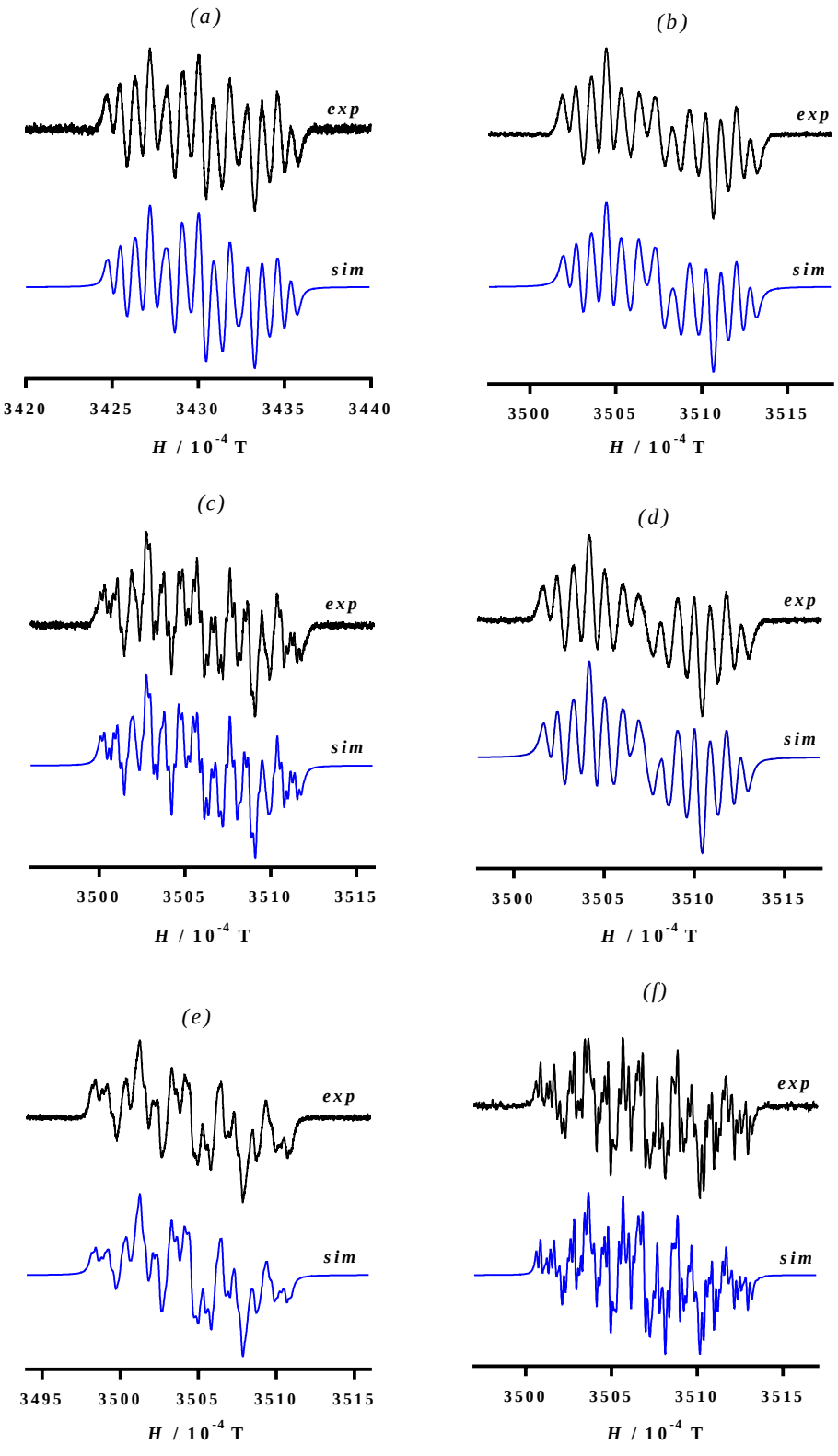
(a)
exp
sim
3420
3425
3430
3435
3440
H / 10-4 T
(b)
exp
sim
3500
3505
3510
3515
H / 10-4 T
(c)
exp
sim
3500
3505
3510
3515
H / 10-4 T
(d)
exp
sim
3500
3505
3510
3515
H / 10-4 T
(e)
exp
sim
3495
3500
3505
3510
3515
H / 10-4 T
(f)
exp
sim
3500
3505
3510
3515
H / 10-4 T

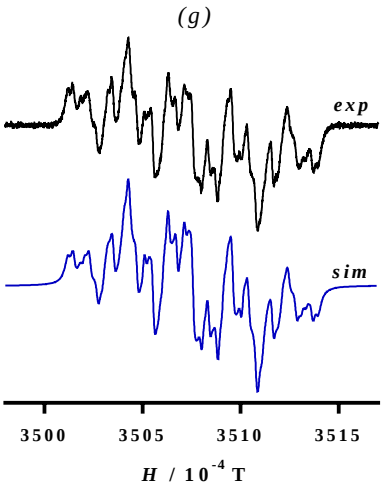


**Figure S8** Experimental (black) and simulated (blue) EPR spectra of RAs in DMF: **2a** (*a*), **2b** (*b*), **2c** (*c*), **2d** (*d*); and in DMF-$H_2O$ ($\chi$=0.462): **2b** (*e*), **2c** (*f*), **2d** (*g*), obtained by stationary electrolysis (298 K) at the first peak potentials of ECR.

## Section 5. Electrochemical detection of DNA duplexes immobilised on Au electrodes

Thin layer electrochemical cell (Figure S9, a) was used for detection. Working electrodes areas were found to be equal 0.09 – 0.11 $cm^2$. Working Au electrodes surface were pre-cleaned in accordance with the procedure described previously[6,7]. The final cleaning of the electrode surfaces was carried out with Kemet diamond polishing paste (UK) followed by cleaning in acetone (1 min) and then twice ultrasonically in twice distilled water for 3 min. Then, to improve a sensitivity of the sensor all working electrodes were modified with microporous golden coating by galvanostatic method (Figure S9, b, c). The galvanic solvent composition: $K[Au(CN)_6]$ (50 mg/5ml) and citric acid (250 mg/5ml), pH=5.5. An average size of porous was found to be 2 μm.

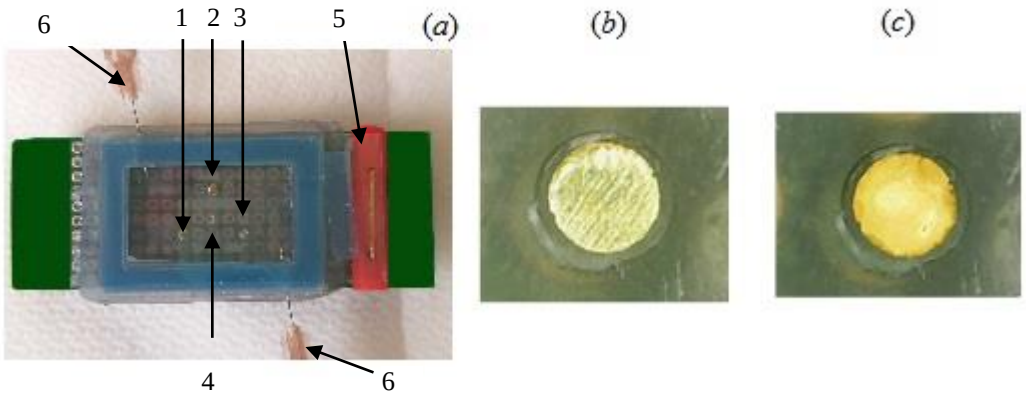


**Figure S9** (*a*) Thin layer electrochemical cell for CV detection of redox active labelled DNA duplexes on Au working electrodes (1-3); 4 – reference Ag disc electrode, 5 – Au wire contact with auxiliary ITO-glass electrode, 6 - buffer input/output syringe needles; microscope images of Au working electrodes: (*b*) before and (*c*) after galvanostatic microporous golden coating.

After galvanostatic modification, the working electrodes were cleaned in distilled water under sonication for 1 min, and then electrochemical "cleaning" of the electrodes was performed in 0.1 M solution of $H_2SO_4$ with a two electrode scheme in the range of potentials $-0.7<E<1$ V until the observed current curves hadn't stopped changing. After "electrochemical cleaning" the cell was sonicated twice for 2 min in mQ water, the working electrode space was dried in a flow of Ar. The working electrodes were immediately modified with 100 μM solution of oligoprobe 1 for 12 h. After modification, the cell was washed twice with stirring in mQ water, dried in an Ar flow, and used immediately for hybridization and CV detection of DNA duplexes.

## Section 6. Hybridization and electrochemical detection of DNA duplexes labelled by 2a,b redox-active modifiers

Hybridization with the oligoprobes **2** was performed on modified electrode 2 (Fig. S9a). Hybridization with a ferrocene labeled oligoprobe (used in our earlier work[3]) was performed on working electrode 1 (Fig. S9a). The hybridization protocol was the same as described earlier[8]. The cell was tightly closed by an ITO-glass auxiliary electrode during the hybridization process. To remove any non-hybridized oligoprobes after hybridization was completed, the working electrodes space was washed with a deoxygenized working buffer (100 mM aqueous solution of $(Et_3HN)HCO_3$, pH=7.2) via syringe needles immersed in the working electrode space (Figure S8a).

CV detection of DNA duplexes was performed immediately after the washing procedure in the same buffer using Metrohm Autolab Potentiostat (Switzerland). CVs were measured using a 3-electrode mode of connecting the cell to the potentiostat. Manual switching between working electrodes was used as described previously[3]. The results of electrochemical detection of DNA duplexes are shown in Fig. 1*b* (see the main text).

## Section 7. Solid state electrochemistry of 2d and confirmation of the origin of electrochemical response of the DNA duplex.

To confirm the origin of the observed electrochemical signal from the DNA duplex (Figure 1 (b), the main text), an additional thin-layer electrochemical experiment was carried out using the adsorption of benzamide **2d** on the working electrode of the sensor. A layer of adsorbed compound **2d** was prepared by precisely dropping of 1mM solution of **2d** in MeCN onto a pre-cleaned and

gold modified electrode 2, followed by drying in an Ar stream. Then, the sensor was washed with a working buffer stream during 30 s, and a CV scan was immediately performed. The resulting CV (Figure S10) showed a signal with a resemble shape as observed for the labelled DNA duplex signal (Figure 1 (*b*), the main text). Both peak potentials coincide, thus proving an origin of the observed DNA duplex response from redox activity of *9H*-thioxanthen-9-one S-dioxide group.

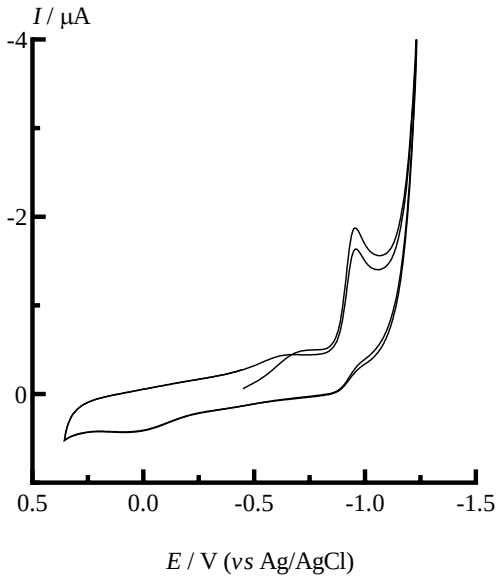


**Figure S10** CV of the adsorbed compound **2d** on the working electrode 2 of the sensor in 100 mM aqueous solution of $(Et_3HN)HCO_3$, pH=7.2.

## Section 8. NMR spectra of thioxanthenones 1a-c and their sulfones 2a-d

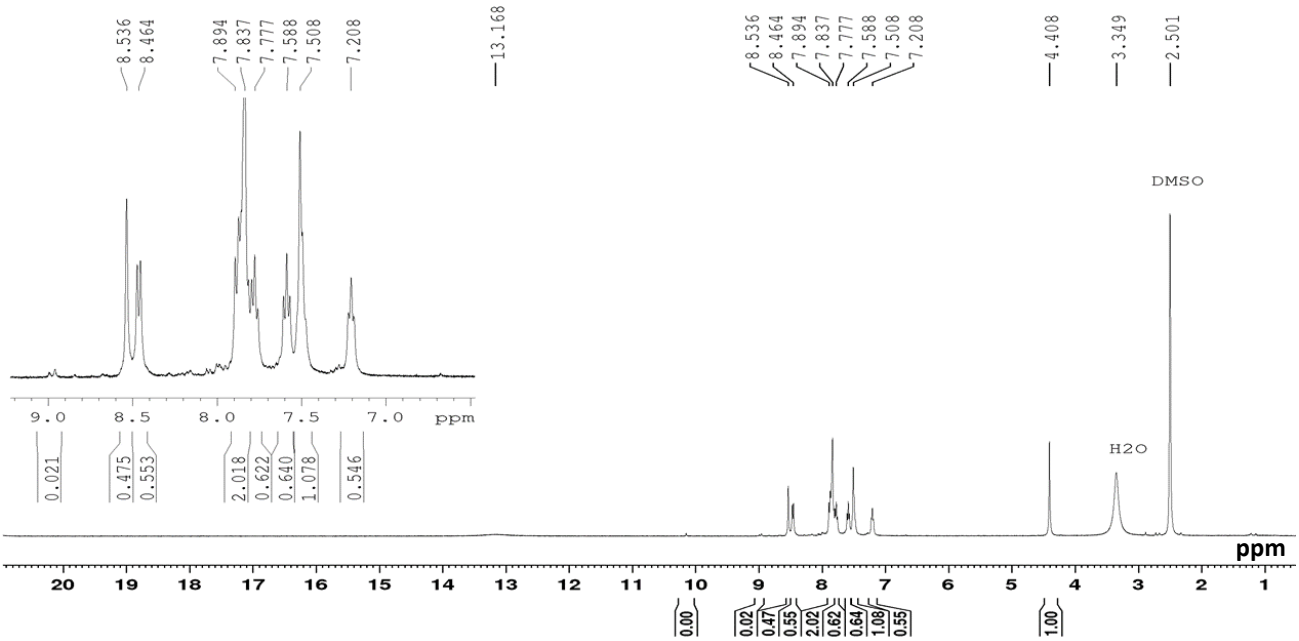


**Figure S11** $^{1}$H NMR spectrum of compound **1a** ($DMSO_{d6}$, 400 MHz, N scans 32)

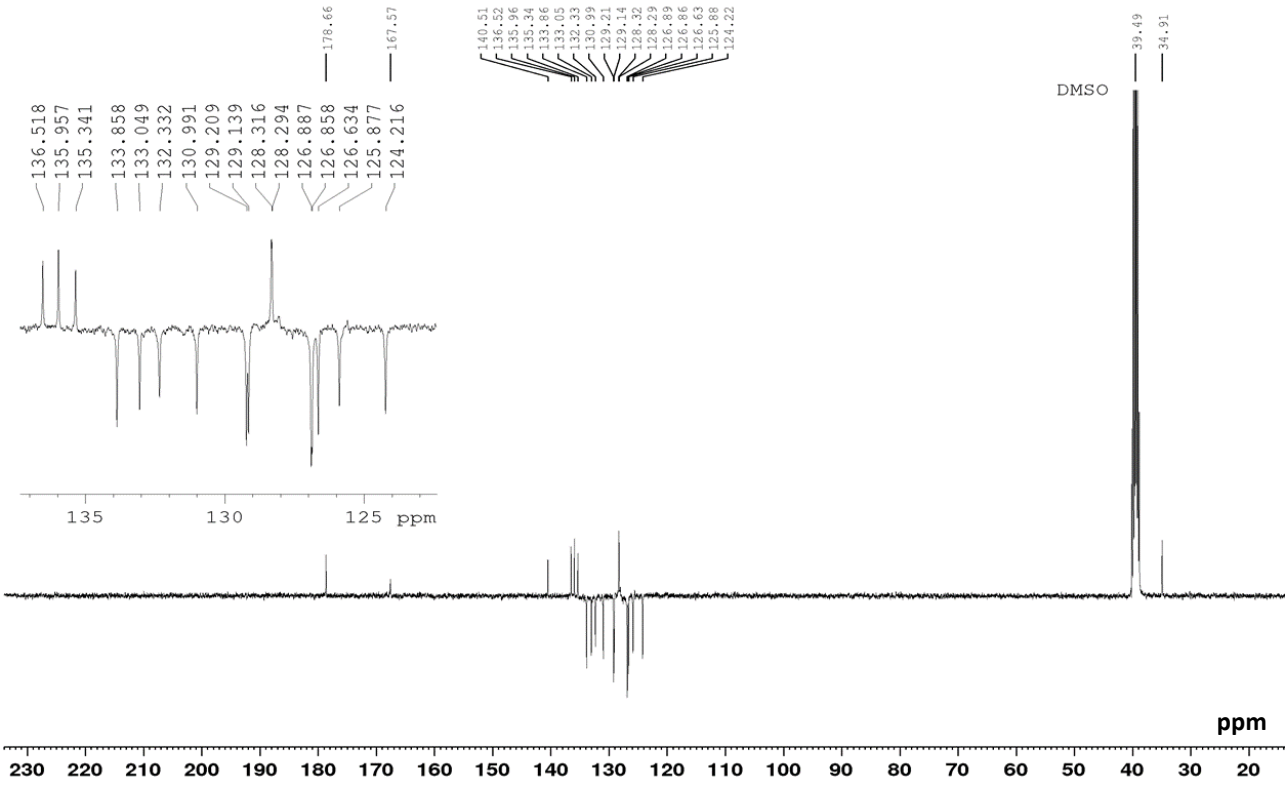


**Figure S12** $^{13}$C NMR spectrum of compound **1a** ($DMSO_{d6}$, 100.6 MHz, N scans 7072)

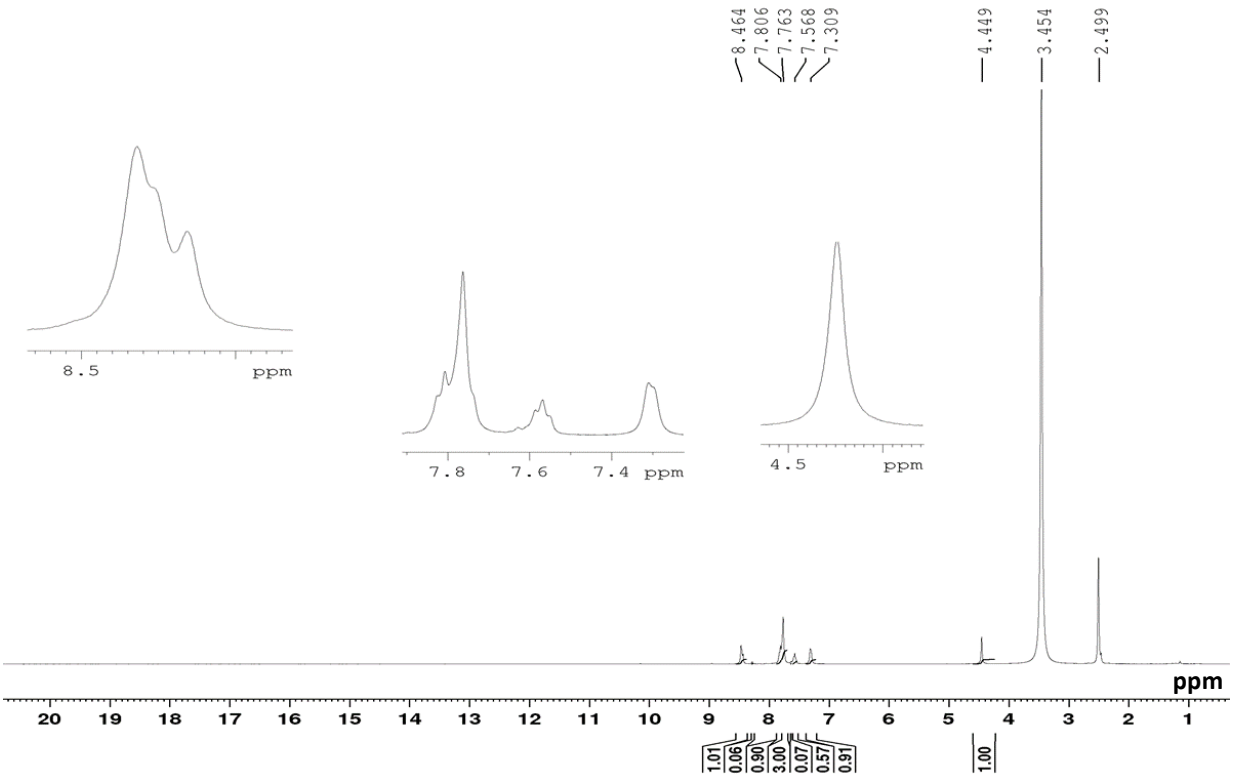


**Figure S13** $^{1}$H NMR spectrum of compound **1b** ($DMSO_{d6}$, 400 MHz, N scans 32)

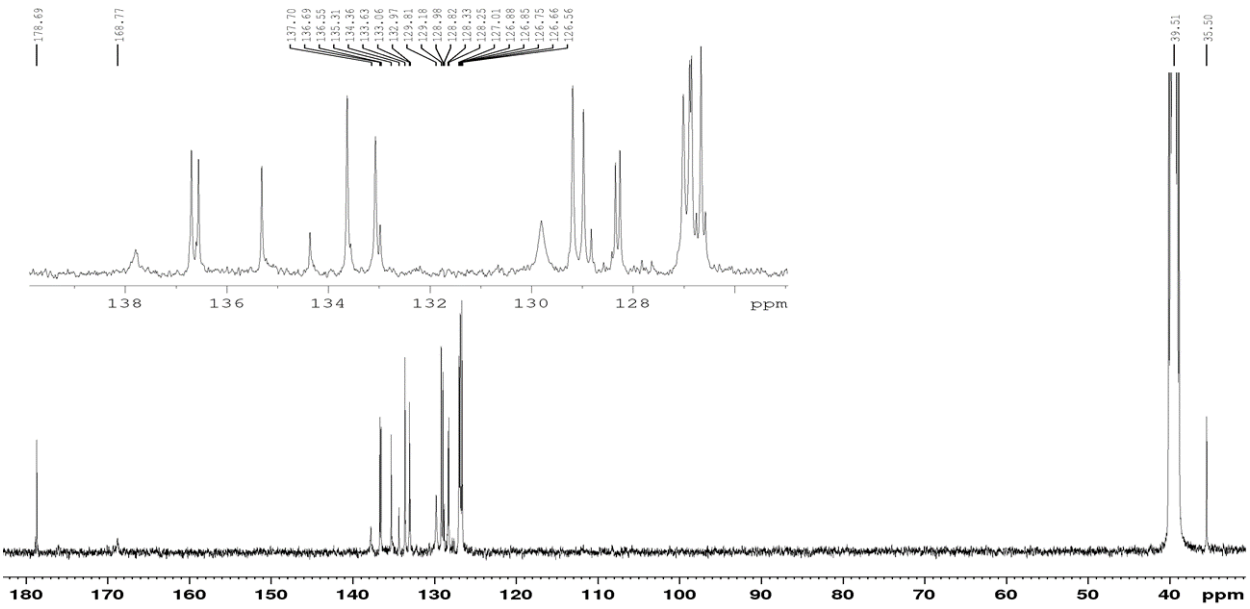


**Figure S14** $^{13}$C NMR spectrum of compound **1b** ($DMSO_{d6}$, 100.6 MHz, N scans 8192)

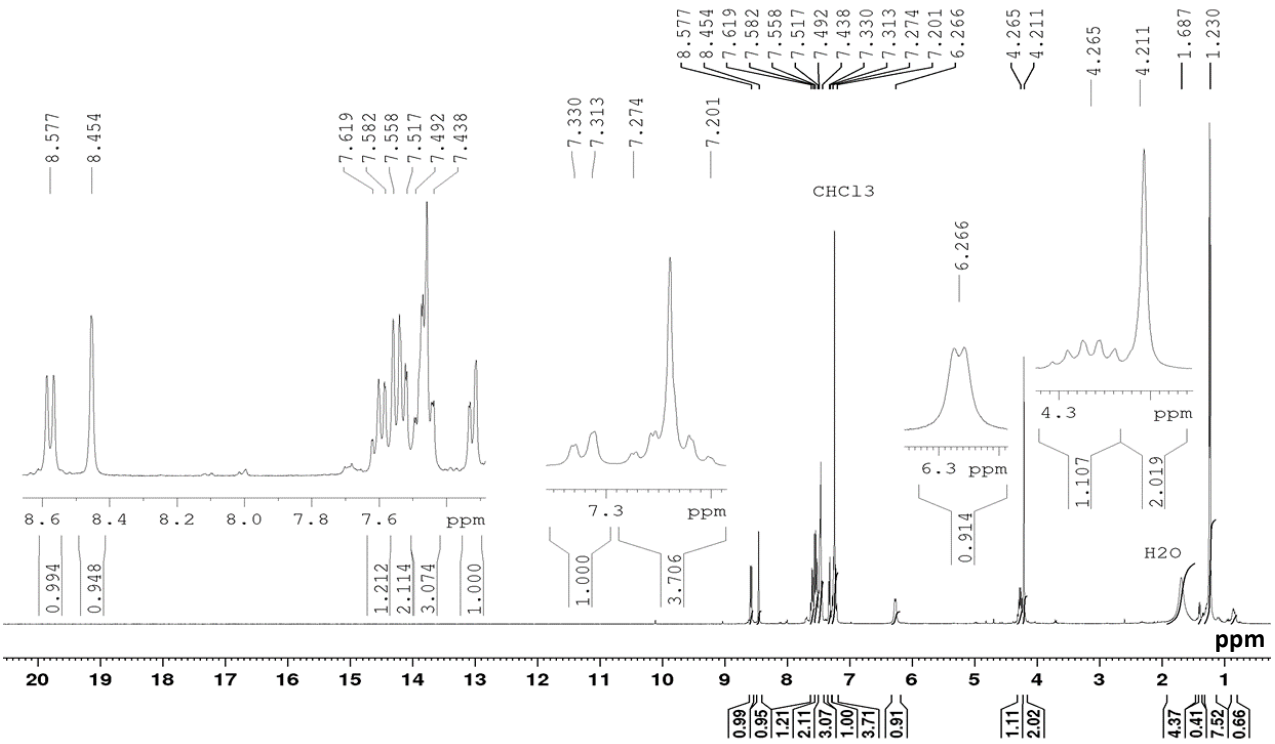


**Figure S15** $^{1}$H NMR spectrum of compound **1c** ($CDCl_3$, 400 MHz, N scans 64)

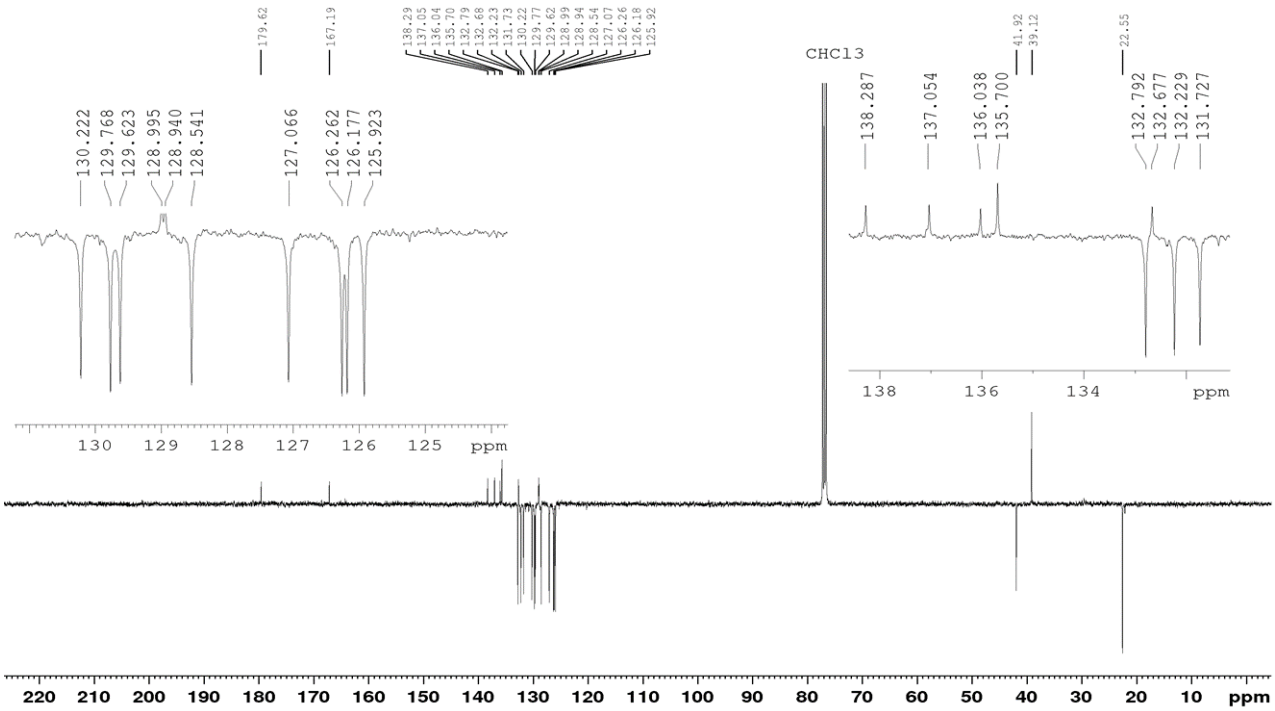


**Figure S16** $^{13}$C NMR spectrum of compound **1c** ($CDCl_3$, 100.6 MHz, N scans 8000)

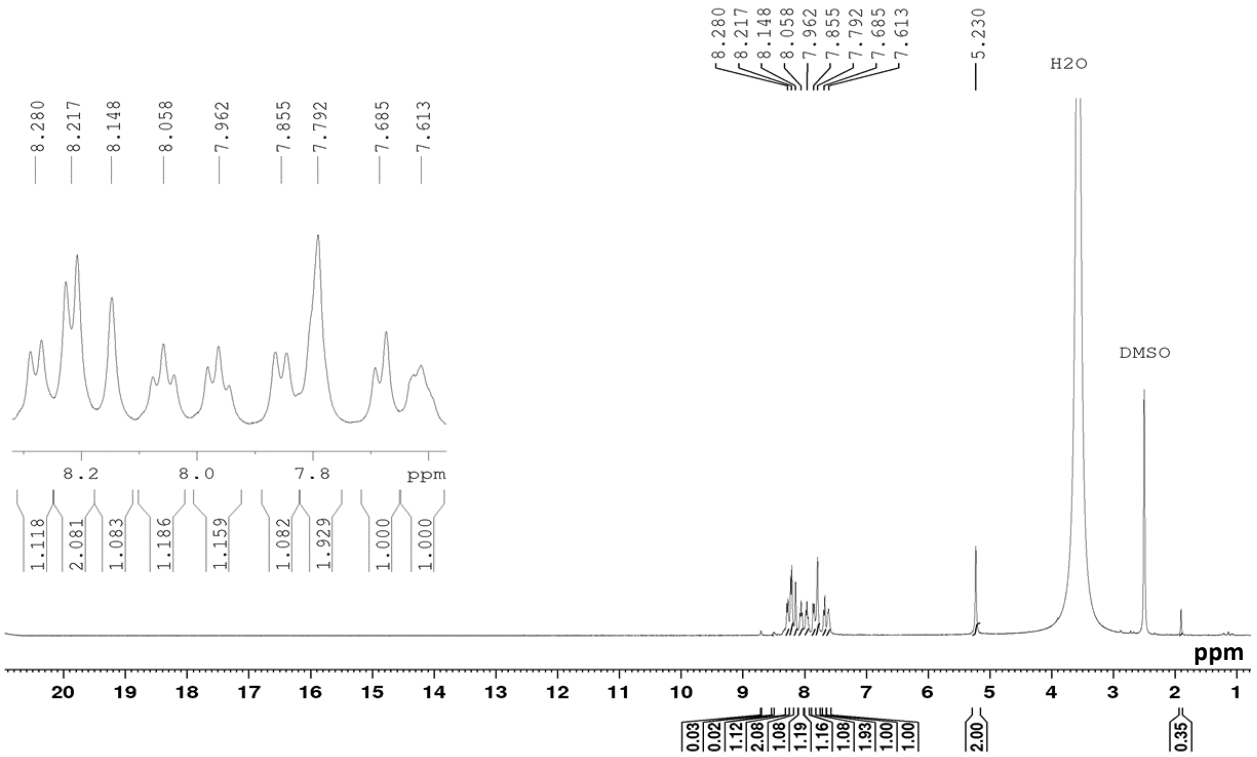


**Figure S17** $^{1}$H NMR spectrum of compound **2a** ($DMSO_{d6}$, 400 MHz, N scans 32)

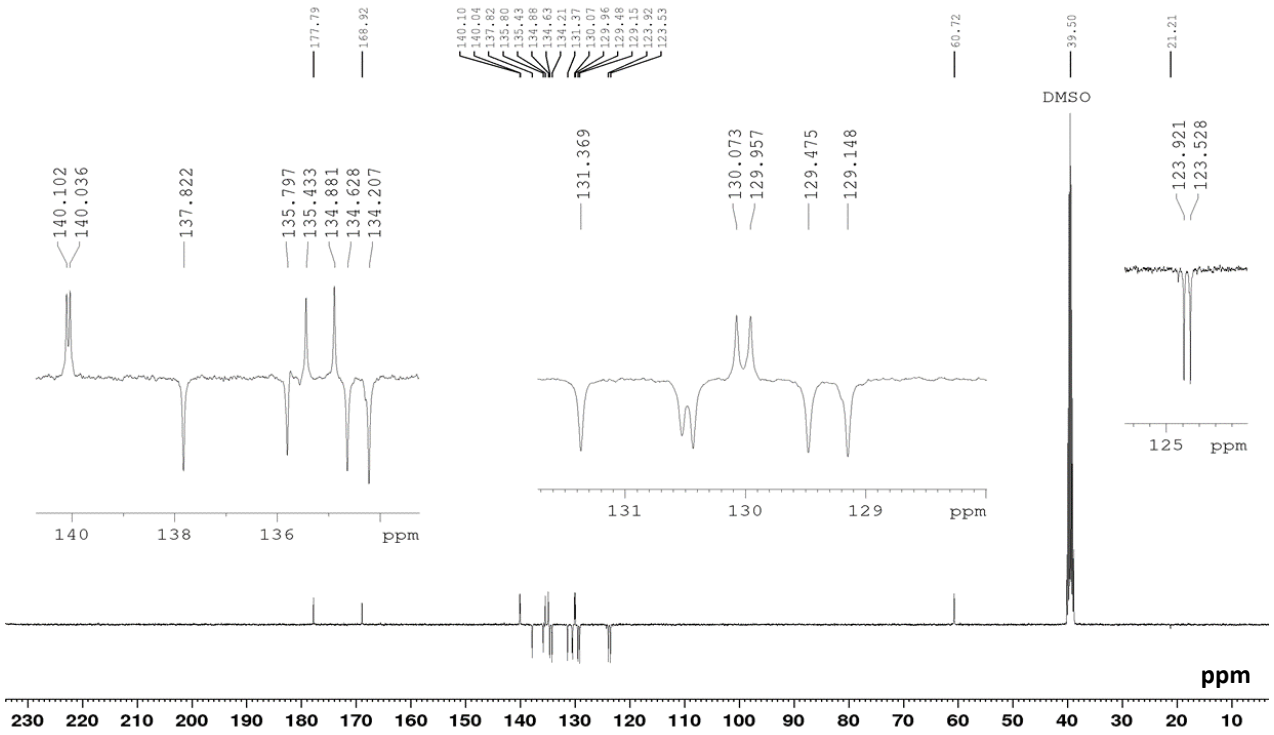


**Figure S18** $^{13}$C NMR spectrum of compound **2a** ($DMSO_{d6}$, 100.6 MHz, N scans 8128)

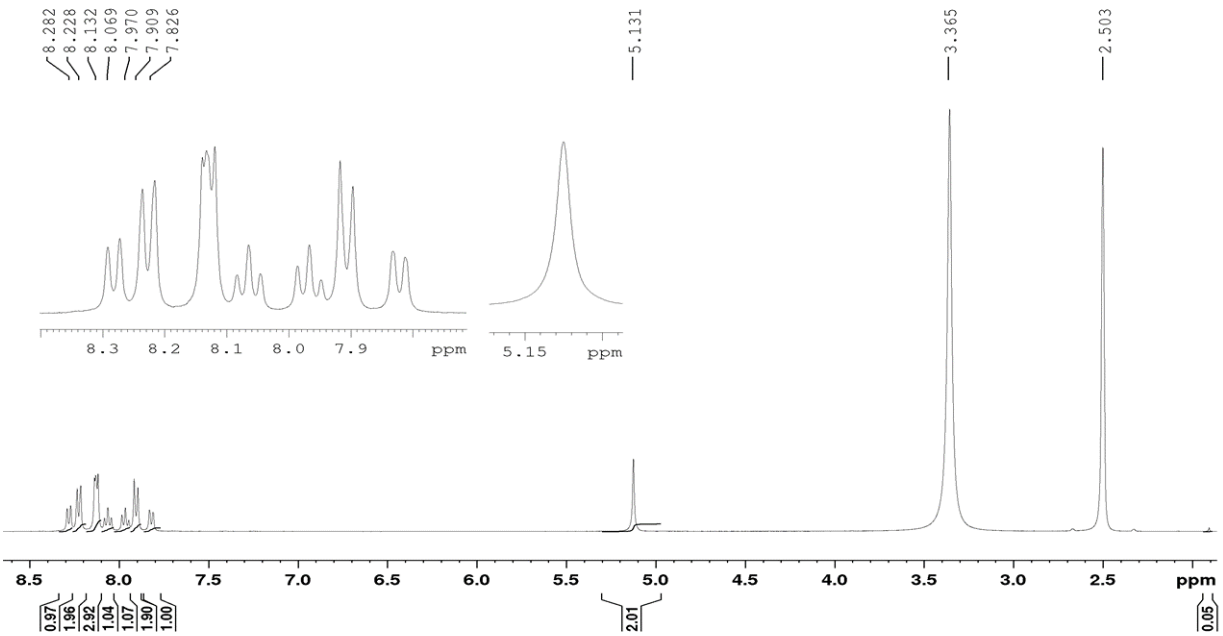


**Figure S19** $^{1}$H NMR spectrum of compound **2b** ($DMSO_{d6}$, 400 MHz, N scans 56)

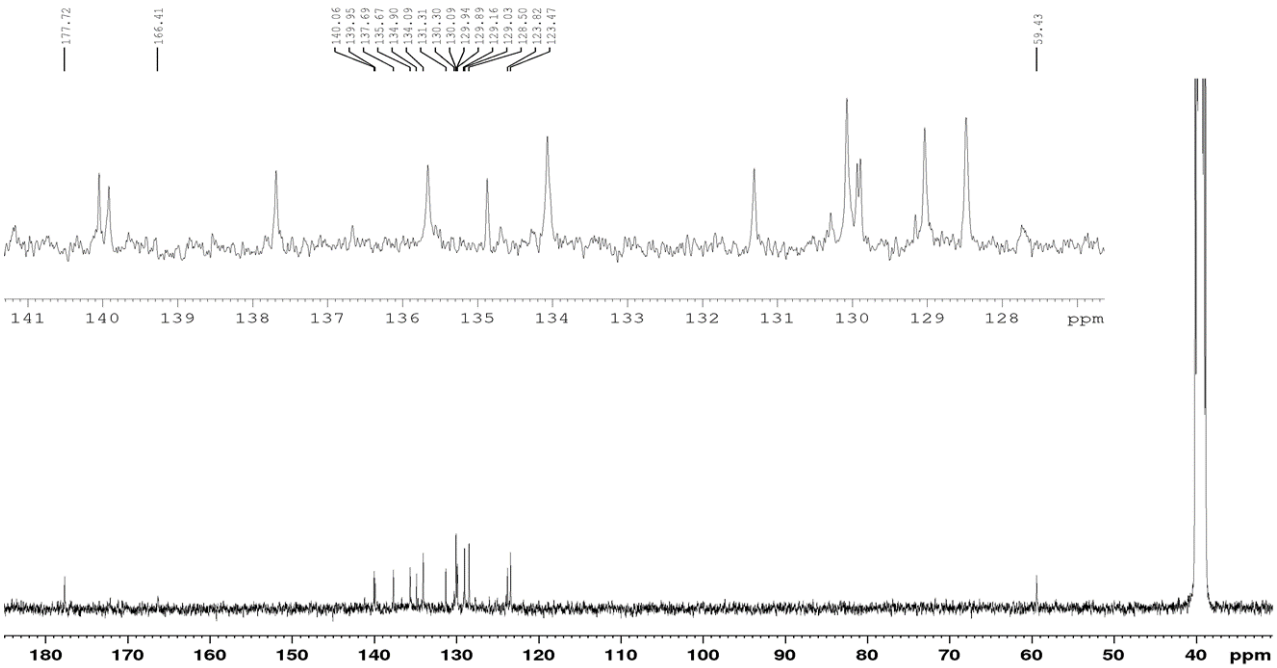


**Figure S20** $^{13}$C NMR spectrum of compound **2b** ($DMSO_{d6}$, 100.6 MHz, N scans 7728)

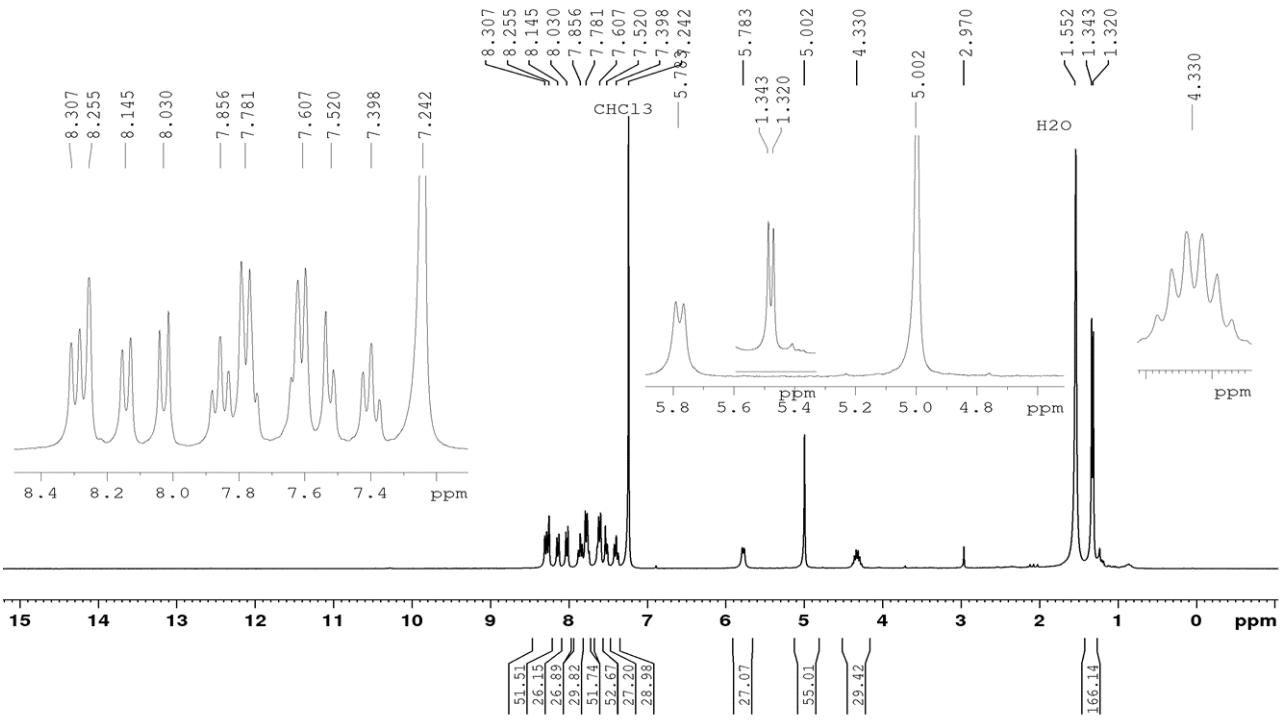


**Figure S21** $^{1}$H NMR spectrum of compound **2c** ($CDCl_3$, 300 MHz, N scans 168)

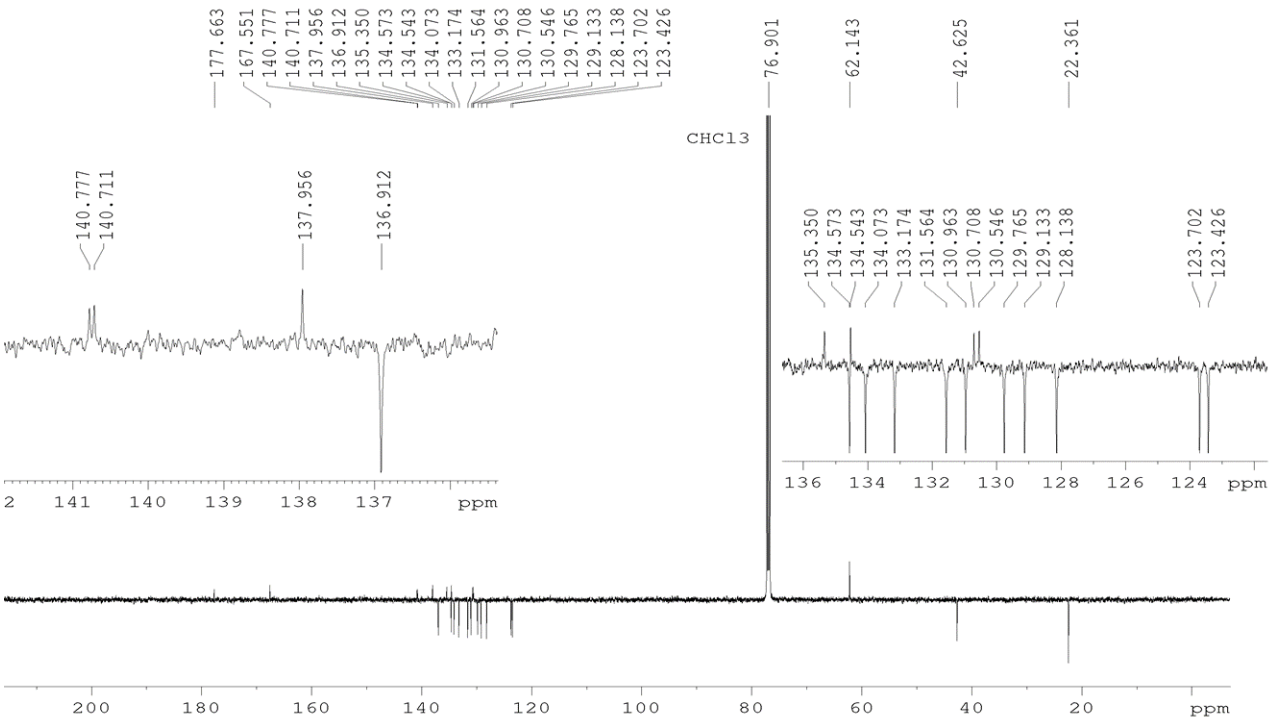


**Figure S22** $^{13}$C NMR spectrum of compound **2c** ($CDCl_3$, 125.8 MHz, N scans 10352)

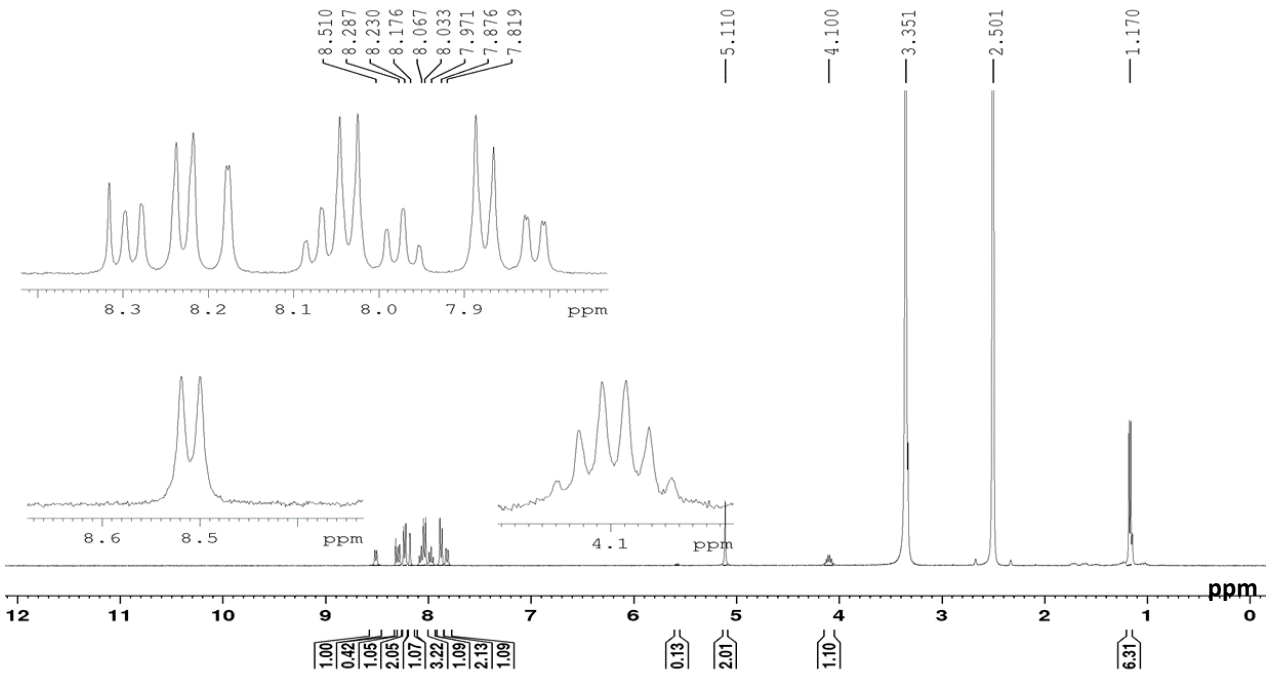


**Figure S23** $^{1}$H NMR spectrum of compound **2d** ($DMSO_{d6}$, 400 MHz, N scans 32)

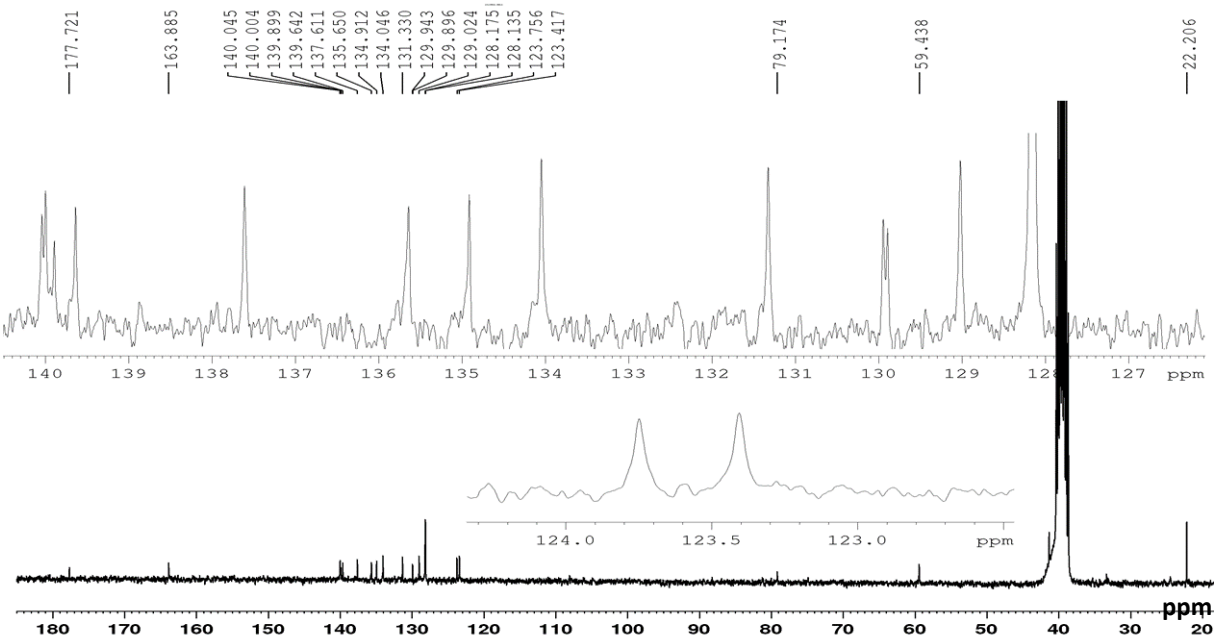


**Figure S24** $^{13}$C NMR spectrum of compound **2d** ($DMSO_{d6}$, 75.5 MHz, N scans 9000)

## References


1 G. Vasiliu, N. Rasanu and O. Maior, *Rev. Chim*., 1968, **19**, 561.

2 V. M. Vlasov and I. A. Os'kina, *Russ. J. Org. Chem.* 2009, **45**, 523.

3 L. A. Shundrin, I. G. Irtegova, N. V. Vasilieva and I. A. Khalfina, *Tetrahedron Lett.*, 2016, **57**, 392.

4 R. D. Duling, *J. Magn. Reson*., 1994, **104**, 105.

5 N. V. Vasilieva, I. G. Irtegova, V. A. Loskutov and L. A. Shundrin, *Mendeleev Commun*., 2013, **23**, 334.

6 D.-W. Pang and H. D. Abruña, *Anal. Chem*., 1998, **70**, 3162.

7 D.-W. Pang and H. D. Abruña, *Anal. Chem*., 2000, **72**, 4700.

8 V. A. Ryabinin, L. A. Shundrin, E. V. Kostina, M. Laassri, V. Chizhikov, S. N. Shchelkunov, K. Chumakov and A. N. Sinyakov, *J. Med. Virol*., 2006, **78**, 1325.